RSC Advances

PAPER

Cite this: *RSC Adv.*, 2015, **5**, 71240

High hydrophilicity and excellent adsorption ability of a stretched polypropylene/graphene oxide composite membrane achieved by plasma assisted surface modification

Jian Dai, Xiao-hao Liu, Yan-jun Xiao, Jing-hui Yang, Peng-kai Qi, Jin Wang, Yong Wang* and Zuo-wan Zhou

In this work, a graphene oxide (GO)-filled polypropylene (PP) adsorptive membrane was developed through an environmentally benign plasma-treatment technology. The PP/GO composite membrane was prepared through melt-compounding and subsequent compression molding processing. The composite membrane was further modified through the plasma treatment with allylamine as the monomer. The results showed that the modified composite membrane exhibited a high hydrophilicity, which is attributed to the introduction of a large number of nitrogen-containing and oxygen-containing groups. The plasma assisted surface modification technology was applied to the porous composite membrane that was prepared through uniaxial stretching processing. Although the porosity of the porous membrane gradually decreased with increasing discharge time during the plasma treatment, the modified porous membrane exhibited an excellent adsorption ability. When adsorbing the particles from the solution, the amount of adsorbed Congo-red particles increased with increasing discharge time. The adsorption mechanism of the treated porous membrane was then analyzed. This work provides an efficient method to apparently improve the hydrophilicity and adsorption ability of a PP-based composite membrane which has great potential in the field of wastewater treatment.

Received 1st June 2015
Accepted 14th August 2015

DOI: 10.1039/c5ra10310j

www.rsc.org/advances

1. Introduction

Wastewater treatment and air purification have attracted extensive attention of researchers in recent years due to the deteriorating water and air pollution. To date, many strategies have been developed to purify the contaminated water or air. Among them, membrane separation or adsorption technology has been proved to be a promising strategy with advantages such as easy operation, high efficiency and low cost, *etc.* As a type of membrane, polymer-based membranes have already been one of the main subjects of much research, and varieties of polymer-based membranes have been successfully prepared and applied in actual wastewater treatment.[1–5] Compared with the other polymer-based membranes, polypropylene (PP) membrane is an appropriate choice for the applications of separation or adsorption due to its good processability, good mechanical property, excellent resistance to chemicals and low cost.[6,7] However, due to the intrinsic hydrophobicity of PP, PP membranes can not be well infiltrated by hydrophilic substances like water and therefore, common PP membranes can not be used in the field of wastewater treatment or in other fields relating to the presence of hydrophilic substances. Enhancing the hydrophilicity of PP membranes becomes vitally important in expanding the application of PP membranes.

Generally, the separation efficiency and/or adsorption ability are the most important parameters for polymer-based membranes when they are used to purify the contaminated water or air. Similar to other polymer-based membranes, the separation efficiency and/or adsorption ability of PP membranes are also influenced by many factors, and among them the most important factors are microstructures and chemical properties of the membranes. The microstructures of PP membranes, including membrane thickness, pore size, porosity and pore connection, can be tailored through adjusting the processing conditions,[8,9] introducing fillers[10,11] or blending with other polymers.[12,13] Obviously, PP membranes with different pore morphologies and/or microstructures exhibit different separation or adsorption efficiencies, which satisfy the different requirements for removing different contaminants. For example, Offord G. T. *et al.*[8] investigated the influence of processing strategies on the permeability of the PP membrane for different gases. The results demonstrated that nitrogen (N_2) flux increased more rapidly than helium (He) flux with

School of Materials Science and Engineering, Southwest Jiaotong University, Key Laboratory of Advanced Technologies of Materials, Ministry of Education of China, Chengdu 610031, P. R. China. E-mail: yongwang1976@163.com; Tel: +86 28 87603042

increasing porosity in this membrane, which resulted in the different selectivity for membranes with different pore indexes. Goodarzi V.[11] prepared PP/ethylene vinyl acetate/clay separation membrane. The membrane exhibited excellent separation ability for oxygen (O_2)/N_2 or carbon dioxide (CO_2)/N_2, and the separation efficiency was dependent on phase morphologies and dispersion states of clay in the membrane.

In terms of chemical properties, they are closely related to the polymer varieties. Due to the differences in intrinsic chemical structure among polymers, there is a great difference among polymers in terms of hydrophilicity, hydrophobicity and interaction with different liquids or particles, which result in different separation efficiencies or adsorption abilities for different polymer membranes.[14,15] PP membrane is a typical hydrophobic membrane and therefore, many methods have been reported to enhance the hydrophilicity of PP membrane, including surface functionalization,[16–18] introducing polar fillers,[19] and blending with other polar polymers[20] *etc.* For example, Xu Q. *et al.*[16] reported that the direct deposition of titanium dioxide (TiO_2) on the surface of the porous PP membrane could enhance the hydrophilicity of the membrane. Similarly, Saffar A. *et al.*[17,20] prepared the modified PP membrane through blending PP with a commercial acrylic acid grafted PP (PP-*g*-AA) and then grafting TiO_2 nanoparticles on the membrane surface. They also found that the hydrophilicity of the modified PP membrane was improved. Furthermore, Chung T. C. *et al.*[21] introduced a hydroxylated PP (PP–OH), which was a very effective surface modifier for PP, into PP matrix. The results demonstrated that the presence of PP–OH provided a hydrophilic surface on the membrane. Consequently, the modified PP membrane exhibited high flux and high retention of substances in the separation process. However, it should be stressed that compared with the common mechanical compounding methods, which exhibit a relatively lower modification efficiency, the surface modification is believed a more effective method to enhance the permeability, separation efficiency and/or adsorption ability.[22–24] Hu M. X. *et al.*[25] investigated the UV-induced graft polymerization of 2-hydroxyethyl methacrylate (HEMA) onto the PP porous membrane and found that the static water contact angle of the membrane surface decreased from 145° to 42° with the grafting degree increasing from 0 to 35.67%, which indicated that the largely enhanced surface hydrophilicity of PP membrane was obtained after surface modification.

Recently, plasma assisted surface modification has been developed to enhance the hydrophilicity of those hydrophobic membranes. Compared with the above-mentioned methods, it seems that plasma treatment is a simpler and more cost-effective method and especially, it has been proved an environmentally benign method[26] that avoids the contamination caused by the usage of various chemicals or solvents during the modification process. This method can introduce certain functional groups on the surface of the substance through energy input, which leads to the cleavage of original chemical bonds and the formation of new chemical bonds between reactive monomers and the matrix. And generally, this method has nearly no influence on intrinsic structures and properties of materials, and only the surface property can be modified according to the application demands.[27–29] For example, Jaleh B. *et al.*[27] investigated the effect of O_2 plasma treatment on the hydrophilicity of PP membrane. It was shown that the contact angle decreased nonlinearly with the treatment time. The drastic change of the oxygen content on the surface showed that the membrane became superhydrophilic due to the significant O_2 implant. Franco J. A. *et al.*[28] prepared the modified PP membrane through the plasma treatment using the poly(tetrafluoroethylene) (PTFE) block as the reactive monomer. It was shown that the modified layer exhibited a negligible resistance to CO_2 mass transfer compared with the bulk PP membrane. The CO_2 mass transfer from gas side into adsorptive liquid for modified PP microporous membrane was greatly enhanced, which was comparable or even superior to the PTFE membrane. Consequently, the highest CO_2 separation efficiency was obtained for the PTFE-treated PP membrane. To further enhance the separation efficiency and/or adsorption ability of modified PP membranes, some novel strategies combining the plasma treatment with other modification methods have been developed. For example, Yang Y. F. *et al.*[29] developed a facile interfacial crosslinking approach, which was combined with a pretreatment by dielectric barrier discharge (DBD) plasma at atmospheric pressure. It was found that the surface hydrophilicity could be significantly enhanced and the durability was also enhanced, which could be demonstrated by the sharp decrease of water contact angle, the double increase of pure water flux and the stability test results. Xu Q. *et al.*[16] prepared the modified PP membrane by depositing TiO_2 on the membrane surface with a pretreatment using plasma. The results demonstrated that after a short exposure to plasma generated in air, oxygen-containing functional groups were formed on the membrane, which was favorable for the deposition of TiO_2 on the membrane surface. Consequently, the deposited membranes showed remarkably enhanced hydrophilicity, which resulted in the simultaneously improved permeability and retention. To date, the plasma-treated PP membranes have already shown great potential in many fields, including biomedical materials, fuel cells, *etc.*,[30,31] however, to the best of our knowledge, rare work is carried out to prepare the modified PP membrane with the aid of plasma treatment for the liquid separation or particle adsorption.

In our previous work, we have successfully prepared PP-based porous membrane containing a small amount of graphene oxide (GO) and/or assistant agent[32] through a uniaxial stretching strategy. The effects of processing conditions on the microstructures and porosities of the composite membranes have been investigated in details. It has been demonstrated that the addition of GO and/or assistant agent can greatly enhance the porosity of the stretched PP membrane. In this work, based on above investigations, the GO-filled composite membrane was firstly prepared under the optimized processing conditions, then the stretched membrane was further treated through plasma assisted surface modification using allylamine as the reactive monomer. The surface hydrophilicity and the adsorption ability of the modified PP composite membrane were comparatively investigated. It was expected that the modified membrane could be used in the field of wastewater treatment.

2. Experimental section

2.1 Materials

PP (trade name of PP140) with a melt flow rate (MFR) of 4.6 g/10 min (190 °C/2.16 kg) was obtained from Kaikai Petrochemical Corporation, China. Graphite was obtained from Qingdao Heilong Graphite Co., Ltd GO was prepared through the oxidation of graphite in our lab according to the modified Hummer's method.[33] After that, some functional groups, including carboxyl and hydroxyl groups, were introduced to the surface of the GO sheets. The corresponding data of the GO can be seen in our previous work and the content of functional groups was about 34.59%.[34] The pore-foaming agent, polyoxyethyleneoctylphenyl-10 (OP-10), was supplied by Chengdu Kelong Chemical Reagent Factory, China. Congo red ($C_{32}H_{22}N_6Na_2O_6S_2$) with the molecule weight of 696.68 g mol^{-1} was supplied by Chengdu Kelong Chemical Reagent Factory, China. The chemical structural formula of Congo red is:

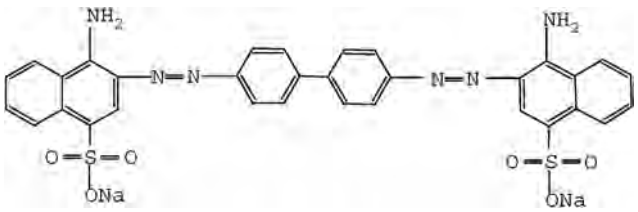

2.2 Preparation of composite membrane

GO and OP-10 were firstly dissolved in the dimethyl formamide (DMF) to improve the dispersion of GO. The homogenous GO/OP-10 solution was poured into PP powder and the mixture was dried at 80 °C for more than 24 h until DMF was completely removed and the weight of sample was invariant. PP/GO/OP-10 composite was then prepared through melt compounding processing, which was conducted on a twin-screw extruder SHJ-20 (Nanjing Ruiya, China) at a screw speed of 200 rpm and the melt temperatures of 150-160-175-190-200-200-195 °C from hopper to die. The contents of GO and OP-10 were maintained at 0.5 wt% and 5 wt%, respectively. After being granulated, the pellets of the composite were compression-molded at a melt temperature of 200 °C and a pressure of 5 MPa to obtain the non-porous composite membrane with a thickness of 0.1 mm. After that, the composite membrane was tailored into dumbbell shape and then stretched to obtain the porous membrane. Stretching was conducted on a universal tensile machine at an environmental temperature of 100 °C. A cross-head speed of 50 mm min^{-1} and a tensile strain of 200% were adopted.

2.3 Plasma treatment for the composite membrane

Both non-porous and porous membranes were modified using plasma treatment technology, which was conducted on a homemade instrument. Allylamine was used as the reactive monomer and argon (Ar) was used as the discharge gas. It has been demonstrated that plasma assisted surface modification using allylamine exhibits relatively higher grafting efficiency compared with the other monomers.[35,36] The base pressure and the monomer gas pressure were kept at 1.0 Pa and 3.5 Pa, respectively. The plasma treatment was conducted at a discharge power of 30 W. In terms of the non-porous membrane, only one side of the membrane was treated for 60 min to make sure that a large amount of functional groups could be grafted on the membrane. For the porous membrane, both sides of the membrane were treated with different discharge time of 0, 10, 30 and 60 min. The corresponding treated membranes were named as M0, M10, M30 and M60, respectively. In comparison, all the characterizations related to the modified layer were carried out with the modified non-porous membrane as the sample in order to eliminate the influence of pores on the measurement. While, to investigate the particle adsorption ability, the porous membranes with different discharge time were used.

2.4 Characterizations

2.4.1 Fourier transform infrared spectroscope (FTIR). A Fourier transform infrared spectroscope (FTIR) spectrometer iS50 (Thermo Nicolet, USA) was used to detect the presence of functional groups on the both sides of non-porous composite membrane. Allowing for absorption coefficient differences with respect to various FTIR bands, a transmission mode with a resolution of 4 cm^{-1} was used. Furthermore, to demonstrate the interaction between modified composite membrane and Congo red particles, the membranes obtained before and after adsorbing Congo red particles were also characterized using FTIR.

2.4.2 X-ray photoelectron spectroscope (XPS). The surface chemical element composition was characterized using X-ray photoelectron spectroscopy (XPS) XSAM800 (Kratos Ltd, UK). The instrument was equipped with a monochromatic Al Kα (1486.6 eV photons) X-ray source. The measurement was carried out at an operating voltage of 12 kV, an operating current of 12 mA and a pressure of 2×10^{-7} Pa.

2.4.3 Atomic force microscopy (AFM). The surface morphology was measured using an atomic force microscope (AFM) CSPM4000 (BenYuan Ltd, China). The contact mode was chosen as the measuring method and the scanning frequency was set at 1 Hz. The 1 μm scanner was chosen and the sensitivity was about 0.03. The membrane sample was tailored into a slice with surface area of 1 cm × 1 cm and placed on the measuring plate. It should be noted that the measuring slice should be placed horizontally.

2.4.4 Contact angle measurement. The hydrophilicity of the membrane surface was evaluated by measuring the static water contact angle. The measurement was conducted on a drop shape analysis system DSA 100(KRÜSS, Germany) at 20 °C. Double-distilled water (H_2O) was used as the probe liquid. Measurements of a given contact angle for both the treated and non-treated surfaces were carried out for at least five times. The non-treated PP and PP/OP-10 non-porous membranes were also measured as comparisons.

2.4.5 Scanning electron microscopy (SEM). A scanning electron microscope (SEM) Fei Inspect (FEI, the Netherlands) was used to characterize the surface morphology of the plasma-treated

membranes and the adsorption of Congo red particles on the membranes. The characterization was carried out at an accelerating voltage of 20.0 kV. Before SEM characterization, all the samples were sputter-coated with a thin layer of gold.

2.4.6 Porosity measurement. The porosity (A_k) of the modified microporous membrane was measured through the following procedures: the membrane was immersed into ethanol for 24 h, after that, the membrane was taken out and the ethanol on the membrane surface was carefully removed using a filter paper. Finally, the wetted membrane was weighted carefully. The porosity was calculated according to the following relation:[37]

$$A_k = \frac{(w_0 - w)\bar{\rho}}{\bar{\rho}w_0 - (\rho - \bar{\rho})w} \times 100\%$$

where w is the initial membrane weight, w_0 is the immersed membrane weight. ρ (0.8 g cm^{-3}) and $\bar{\rho}$(0.91 g cm^{-3}) are the density of ethanol and PP, respectively.

2.4.7 Particle adsorption measurement. The particle adsorption measurement was carried out through the immersing method with Congo red as the probe particle. The Congo red was firstly dissolved in the ethanol to form the homogenous solution with the concentration of 1 mg ml^{-1}. Then, the porous membranes with the same surface area and different discharge time were immersed into the solution for 3 days. Meanwhile, the solution without membranes was also prepared as a comparison. After that, the porous membranes were taken out and the residue amount of Congo red in the solution was detected using a UV-Vis Spectroscope UV-1800PC (SPECTROPHOTOMETER, Japan). The detecting wavelength range was 400 to 700 nm.

2.4.8 Wide angle X-ray diffraction. To further demonstrate the adsorption of Congo red particles on the porous membranes, the composite membranes obtained before and after adsorbing Congo red particles were also characterized using a wide angle X-ray diffraction (WAXD) DX-1000 (Dandong Fangyuan Instrument, China). The continuous scanning angle (2θ) range used in this study was from 5° to 40° at 35 kV and 25 mA.

3. Results and discussion

3.1 Evaluation of plasma assisted surface modification

In this section, all the samples that were selected for comparatively studying the effect of plasma assisted surface modification on microstructure and hydrophilicity of membranes were non-porous membranes. The chemical structures of the compression-molded membrane surfaces with and without plasma treatment were firstly detected using FTIR. Fig. 1 shows the corresponding FTIR spectra of samples. It can be seen that compared with the non-treated sample, the plasma-treated sample exhibits at least two changes in FTIR spectrum. Firstly, it exhibits several characteristic absorption bands with higher absorption intensities at wavenumbers of about 1625, 1650, and 3200–3400 cm^{-1}, which are attributed to the stretching vibration of –NH_2 group, the stretching vibration of the C=NH group, and the stretching vibration of the –NH_2 and the –OH groups, respectively.[38] This indicates that a number of N- and O-containing groups were successfully introduced on the PP membrane surface through the degradation of allylamine and subsequent grafting reaction during the modification process. Secondly, compared with the non-treated sample, the plasma-treated sample exhibits relatively lower intensity of the characteristic absorption bands at about 2800–3000 cm^{-1}, which are attributed to the stretching vibration of –CH_2 groups in the PP chain backbones. This demonstrates that the surface of the treated sample is covered by the deposited layer to a certain extent.

For more evidences of the surface modification, XPS was also employed to confirm the functionalization effect of the PP composite membrane. Fig. 2a shows the wide scan of XPS spectra of non-treated and treated PP membranes. It can be seen that for the non-treated PP composite membrane, the C 1s and O 1s are major components, and the corresponding atomic concentrations are 76.66% and 18.61%, respectively. It is believed that O element derives from the functional groups of GO and OP-10. After the plasma treatment, besides the presence of C and O elements, one can observe a definite peak at binding energy of about 399.5 eV, which is attributed to the presence of N element. The atomic concentration of N 1s component is about 7.64%. This further demonstrates that some N-containing groups are introduced onto the PP composite membrane surface. Furthermore, compared with the non-treated sample, one can also see that the atomic concentration of C 1s is slightly decreased while the atomic concentration of O 1s maintains nearly invariant.

In order to better understand the principal functional groups on the plasma-treated PP composite membrane surface, high resolution XPS analyses of C 1s, N 1s and O 1s peaks were carried out. The concentration of each chemical component can be calculated by deconvolution using Gaussian–Lorentzian fitting technology. Fig. 2b–d show the high resolution XPS spectra of C 1s, O 1s and N 1s of PP composite membranes before and after being treated, respectively. The corresponding data are listed in Table 1. It can be seen that for C 1s spectra (Fig. 2b), the non-treated PP composite membrane exhibits at least three peaks with binding energy of 284.6, 285.5 and 288.0 eV, which are attributed to the presence of C–C/C–H/C=C, C–OR/C–N–C/C=N–C, and C=O/C–N–O/C=N/C≡N,[38–40] respectively. After being treated, the modified PP composite membrane still exhibits the three peaks at 284.6, 285.9 and 286.9 eV. Compared with the XPS spectra of non-treated sample, there are several changes that need to be pointed out for the treated sample. Firstly, the peak intensity at 284.6 eV decreases while the peak intensity at 285.9 eV increases, which indicate that PP chains are partially covered by the deposition substances. Secondly, the peak at 288.0 eV shifts to lower binding energy (286.9 eV) but the intensity slightly increased, which indicate the disappearance of C=O/C–N–O and the increased concentration of C=N/C≡N.[38,39] In terms of N 1s spectra (Fig. 2c), it is hardly to detect the presence of N element on the surface of non-treated PP composite membrane. However, the treated sample exhibits several peaks at 398.8, 399.8 and 400.8 eV, which are attributed to the presence of C–N/C=N, C≡N/–N–C=O/N–CO–N, and O–CO–N/CO–N–CO/C–NH_3^+,[38]

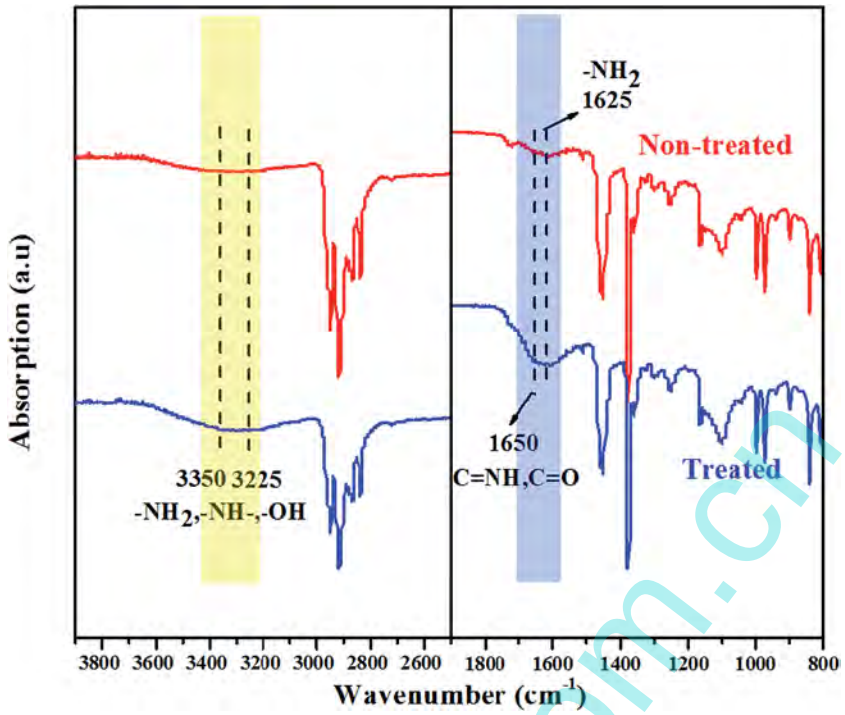

Fig. 1 FTIR spectra of non-treated composite membrane and treated PP composite membrane obtained after plasma assisted surface modification for 60 min. Non-porous composite membranes were used.

respectively. This further demonstrates that some N-containing groups are introduced onto the PP composite membrane surface through plasma treatment. For O 1s spectra (Fig. 2d), the non-treated sample exhibits peaks at 531.5, 532.3 and 532.9 eV, which are attributed to the presence of N–C=O/O–C–O/N–CO–N, C=O/C–O–C, and C–O–C (aromatic),[39] respectively. After being treated, the intensity of the first peak decreases while the peak position maintains invariant. However, the latter two peaks shift to higher binding energies (532.4 and 533.2 eV) with higher intensity, which indicates that the content of C=O and C–O–C groups increases to some degree on one hand. On the other hand, the variations also indicate the presence of a few –OH groups on the treated PP composite membrane.[39] From the variations in content of all components as shown in Table 1, it can be deduced that some of the C–C/C–H/C=C bonds in the membrane surface may be broken by the plasma treatment, and the broken bonds recombine with N or O atoms that are produced by N- and O-containing groups, which results in the connection of functional groups with the molecular chain of composite membrane surface.[35] In other words, the composite membrane is successfully modified through the plasma assisted surface modification technology using allylamine as the reactive monomer.

Fig. 3 shows the variation of membrane surface roughness before and after plasma treatment. For the non-treated sample, the surface roughness is about 10.5 nm. After being treated, the surface roughness is decreased to 9.1 nm. This indicates that the plasma treatment can reduce the surface roughness to a certain degree. Based on the Density Functional Theory (DFT) proposed by Hohenberg,[41] the average energy needed for breaking the chemical bonds of GO and PP chains was calculated. The results demonstrate that a relatively higher average energy of about 5.368 eV is required for breaking the C–C bonds of GO, while a relatively lower average energy of about 4.592 eV is required for breaking the C–C bonds of PP chains. This suggests that the grafting reaction occurs mainly on the PP chains and a modified layer is easier to be deposited on the region that is rich in PP chains. Namely, a thicker modified layer is deposited on PP compared to GO. Consequently, the composite membrane surface is smoothed.

Generally, the introduction of polar functional groups on the surface of the hydrophobic sample leads to the enhancement of the hydrophilicity and correspondingly, the enhanced hydrophilicity is usually used to demonstrate the functionalization of the hydrophobic sample. The hydrophilicity of sample surface can be evaluated by measuring the static water contact angle. In the present work, the static water contact angles on the PP composite membrane surface before and after plasma treatment were measured. As is known to all, PP membrane is highly hydrophobic. However, from Fig. 4a one can see that the composite membrane shows good hydrophilicity with a contact angle of 29.5°, which is much smaller than the 68.8° and 68.2° of neat PP and PP/OP-10 membranes (not shown here), respectively. Obviously, the enhanced hydrophilicity of composite membrane is mainly attributed to the presence of GO particles with many polar groups, including carboxyl and hydroxyl groups. Adding GO particles to improve the hydrophilicity of polymer materials has been reported elsewhere.[42,43] After the plasma treatment, the treated sample exhibits very small contact angle (Fig. 4b) of only 11.9°, which is even comparable to the lowest contact angle of the modified PP

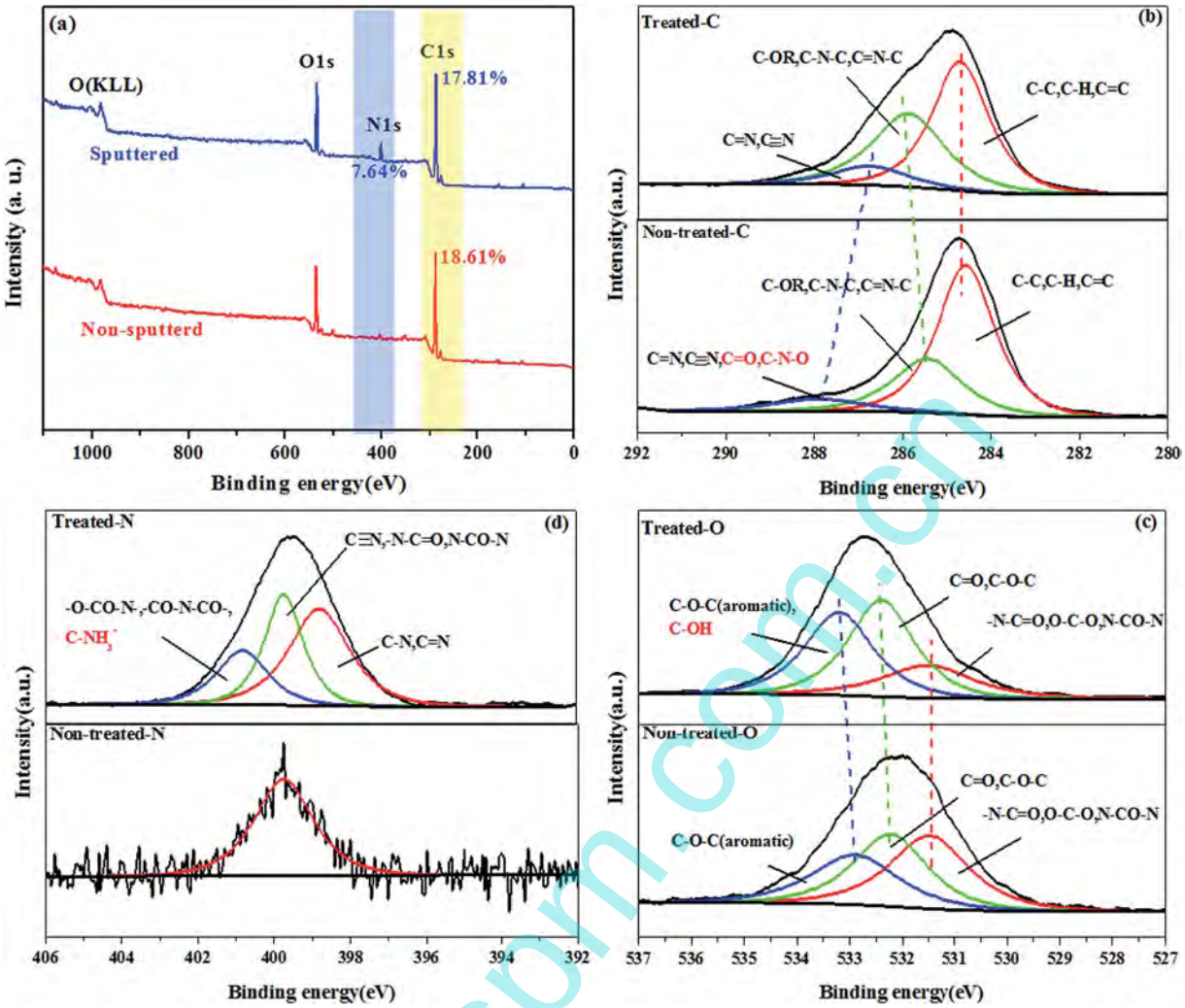

Fig. 2 (a) XPS wide scan spectra of non-treated PP composite membrane and treated PP composite membrane obtained after plasma assisted surface modification for 60 min, (b–d) showing the comparison of spectra for C 1s, N 1s and O 1s between non-treated and treated PP membranes, respectively. Non-porous composite membranes were used.

porous membrane reported in the literature.[18] This indicates that a composite membrane with high hydrophilicity is obtained in this work. Therefore, it can be deduced that a kind of high-hydrophilic membrane is successfully prepared through plasma assisted surface modification of the PP-based composite membrane with the addition of GO, which is generally regarded as a kind of non-polar or hydrophobic membrane. And the hydrophilicity is apparently enhanced mainly due to the

Table 1 Details of binding energy and relative contents of different functional groups calculated from XPS curves

	Non-treated		Treated		
Element	Content	Binding energy (eV)	Content	Binding energy (eV)	Functional groups
C 1s	66.1%	284.6	57.2%	284.6	C–C, C–H, C=C, C–OR, C–N–C, C=N–C,
	25.9%	285.5	33.9%	285.9	C=C, C≡C, C=O, C–N–O
	8.0%	288.0	9.9%	286.9	
O 1s	37.8%	531.5	25.4%	531.4	–N–C=O, O–C–O, N–CO–N, C=O,
	34.5%	532.3	41.7%	532.4	C–O–C, C–O–C (aromatic), C–OH
	27.7%	532.9	32.9%	533.2	
N 1s	—		43.2%	398.8	C–N, C=N, C≡N, –N–C=O, N–CO–N,
			37.6%	399.8	–O–CO–N–, –CO–N–CO–, $C–NH_3^+$
			19.2%	400.8	

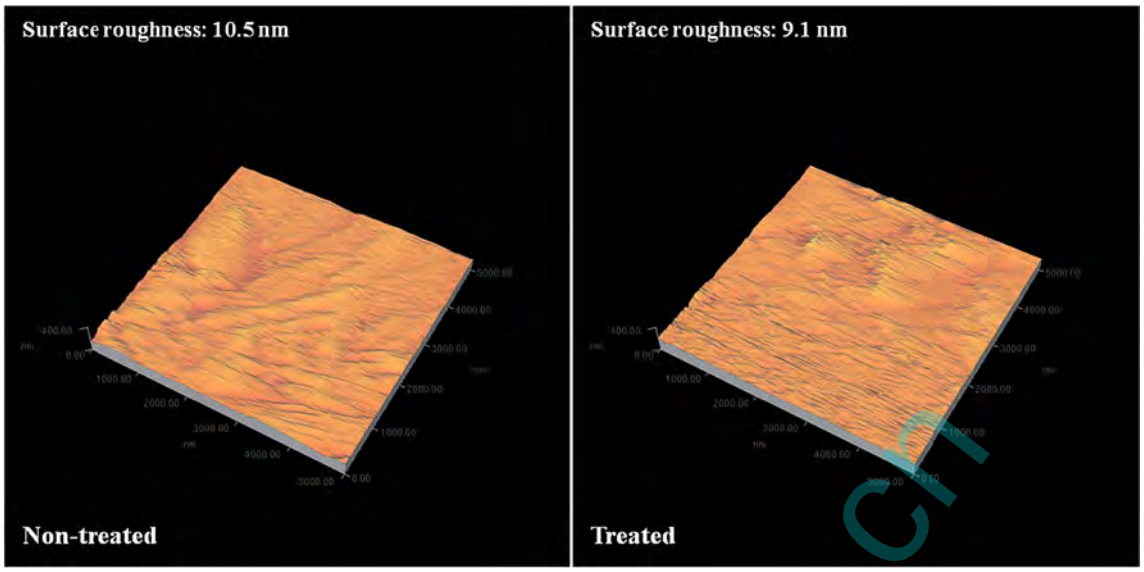

Fig. 3 AFM images of non-treated and treated PP composite membrane obtained after plasma assisted surface modification for 60 min. Non-porous composite membranes were used.

presence of a large amount of functional groups, which also endow the membrane with a great potential in the application of separation and/or adsorption.

3.2 Particle adsorption ability of plasma treated porous composite membrane

The PP-based porous composite membrane can be easily prepared through the stretching strategy. As the tensile stress is applied, the lamellae separation happens, which results in the formation of pores. The pore parameters can be well-controlled through adjusting the tensile parameters.[8,9] In our previous work,[32] the PP-based porous composite membrane with high porosity has been successfully prepared through adjusting the tensile conditions and introducing GO. However, the absence of enough functional groups on the membrane surface limits the application of PP-based porous composite membrane in more fields. To seek a possible application for liquid separation and/or particle adsorption, the PP-based porous composite membrane that obtained through stretching process is further treated through the plasma assisted surface modification as demonstrated above.

In the present work, the treated porous composite membranes were obtained with different plasma discharge time. The effect of plasma treatment on the pore morphology of the composite membrane was firstly investigated using SEM and the representative SEM images are shown in Fig. 5. For the non-treated porous composite membrane (Fig. 5a), a large amount of pores are observed on the stretched membrane surface, which is mainly attributed to the breakage and/or separation of lamella during the tensile process.[44,45] For the treated porous membranes, there are at least two features that need to be noticed. Firstly, the number of the pores decreases with increasing discharge time. This can be attributed to the deposition of modified layer that covers the small pores. Obviously, increasing discharge time leads to thicker modified layer and consequently, more pores are covered. Specifically, when the discharge time is increased up to 60 min, a very thick modified layer is deposited on the membrane surface and most

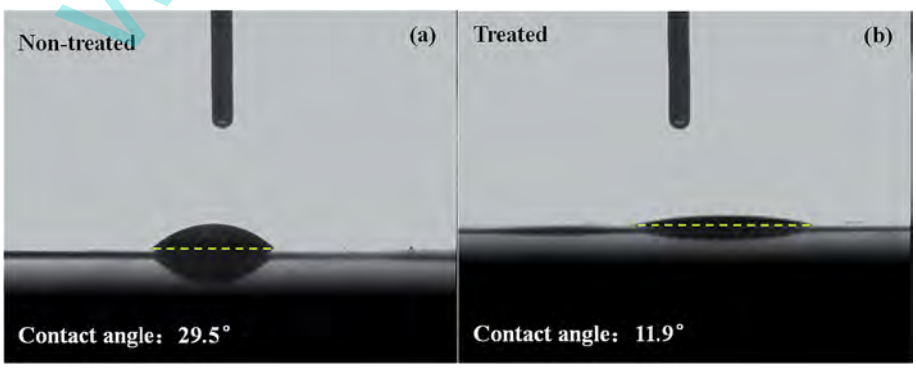

Fig. 4 Pictures of non-treated and treated PP composite membrane obtained from contact angle measurement. Non-porous membranes were used. The treated PP composite membrane was obtained after plasma assisted surface modification for 60 min.

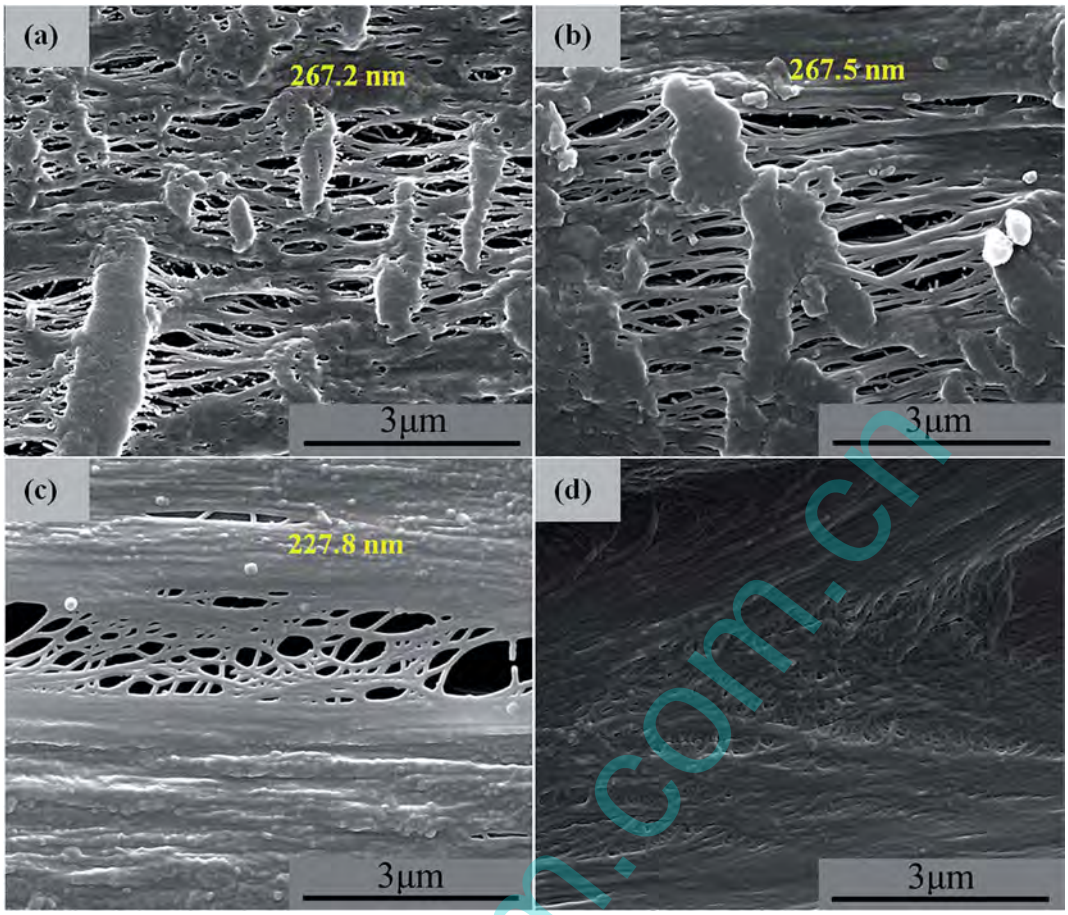

Fig. 5 SEM images showing the surface morphologies of (a) M0; (b) M10; (c) M30; (d) M60. The average pore sizes were calculated and shown in the images.

of the pores are covered. The average pore size was also calculated by measuring at least 200 pores from different zones of the membrane according to the Nano Measurer 1.2 software. It can be seen that before plasma treatment (M0), the average pore size is about 267.2 nm. Although the M10 membrane exhibits very similar average pore size to that of the M0 membrane, the M30 membrane exhibits apparently decreased average pore size (227.8 nm), demonstrating the decrease of the pore size induced by plasma treatment. For the M60 membrane, it is very difficult to calculate the average pore size because most of pores are covered by the deposited layer and therefore, the average pore size is not provided. Secondly, the surface roughness decreases and the membrane surface becomes smoother with increasing discharge time during the plasma treatment.

The variation of porosity with the discharge time is shown in Fig. 6. It can be seen that the porosity decreases monotonously as the discharge time increases. The non-treated porous membrane surface exhibits a porosity of about 22.1%. After being treated for 10 min, the porosity is decreased to 13.4%. As the discharge time increases up to 60 min, the treated membrane becomes non-porous and nearly no pores can be detected. Obviously, it is believed that the porosity of the stretched membrane can be well-adjusted in a wide range by controlling the discharge time.

The particle adsorption ability was measured with the Congo red as the probe particles. The appearances of membranes, which were immersed in ethanol for 3 days and dried, were

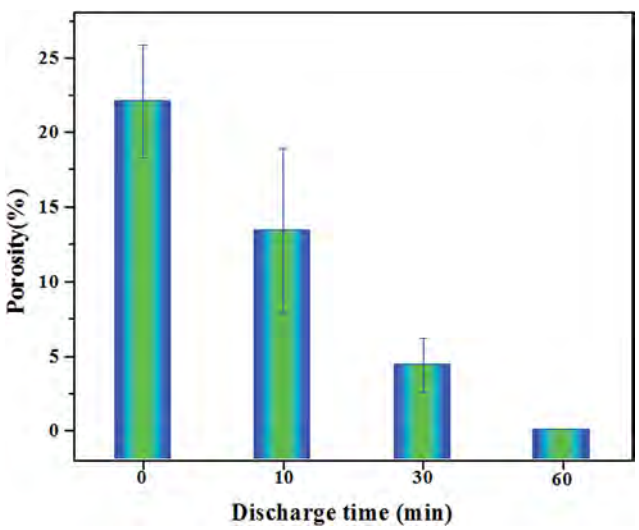

Fig. 6 Variations of porosity of PP porous composite membranes *versus* the discharge time.

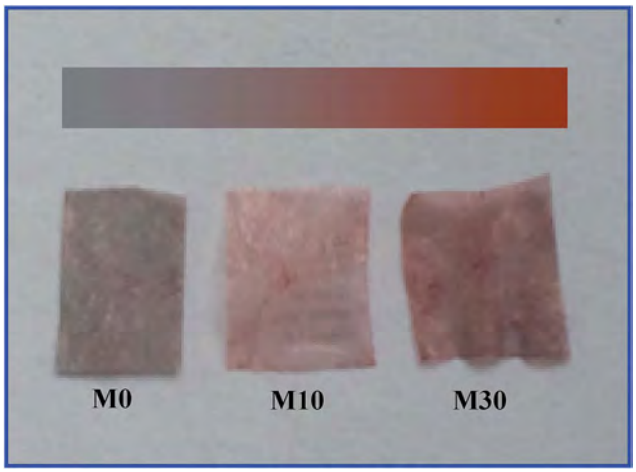

Fig. 7 The photograph showing the macro morphologies of PP composite membranes with different discharge time after adsorption.

taken photos. As shown in Fig. 7, the color becomes deeper and deeper as the discharge time increases, which clearly indicates that more Congo red particles are adsorbed on the membrane surface. To further demonstrate the adsorption of Congo red particles on the surface of porous composite membrane, the surface morphologies of all the membrane samples were characterized using SEM as shown in Fig. 8. From Fig. 8a one can see that only a few of tiny particles are adsorbed on the surface of the non-treated membrane (M0), indicating the weak adsorption ability for the nascent PP composite membrane. The adsorption of Congo red particles may be ascribed to the interaction between amino groups ($-NH_2$) of Congo red and polar groups of GO and/or OP-10 in the composite membrane. For the treated membranes (Fig. 8b and c), it can be seen that amounts of Congo red aggregates with larger particle size are adsorbed on the membrane surface. On one hand, there are many O-containing groups existing on the membrane surface, such as –OH or amide group ($-CONH_2$), which can directly interact with the $-NH_2$ groups of Congo red particles. On the other hand, the N-containing groups on the membrane surface can interact with the ethanol solvent, which weakens the interaction between the $-NH_2$ groups of Congo red and the ethanol solvent. Furthermore, there is a possible π–π stacking interaction between the aromatic structure of Congo red and hexatomic ring of GO with sp^2 hybrid structure, which also

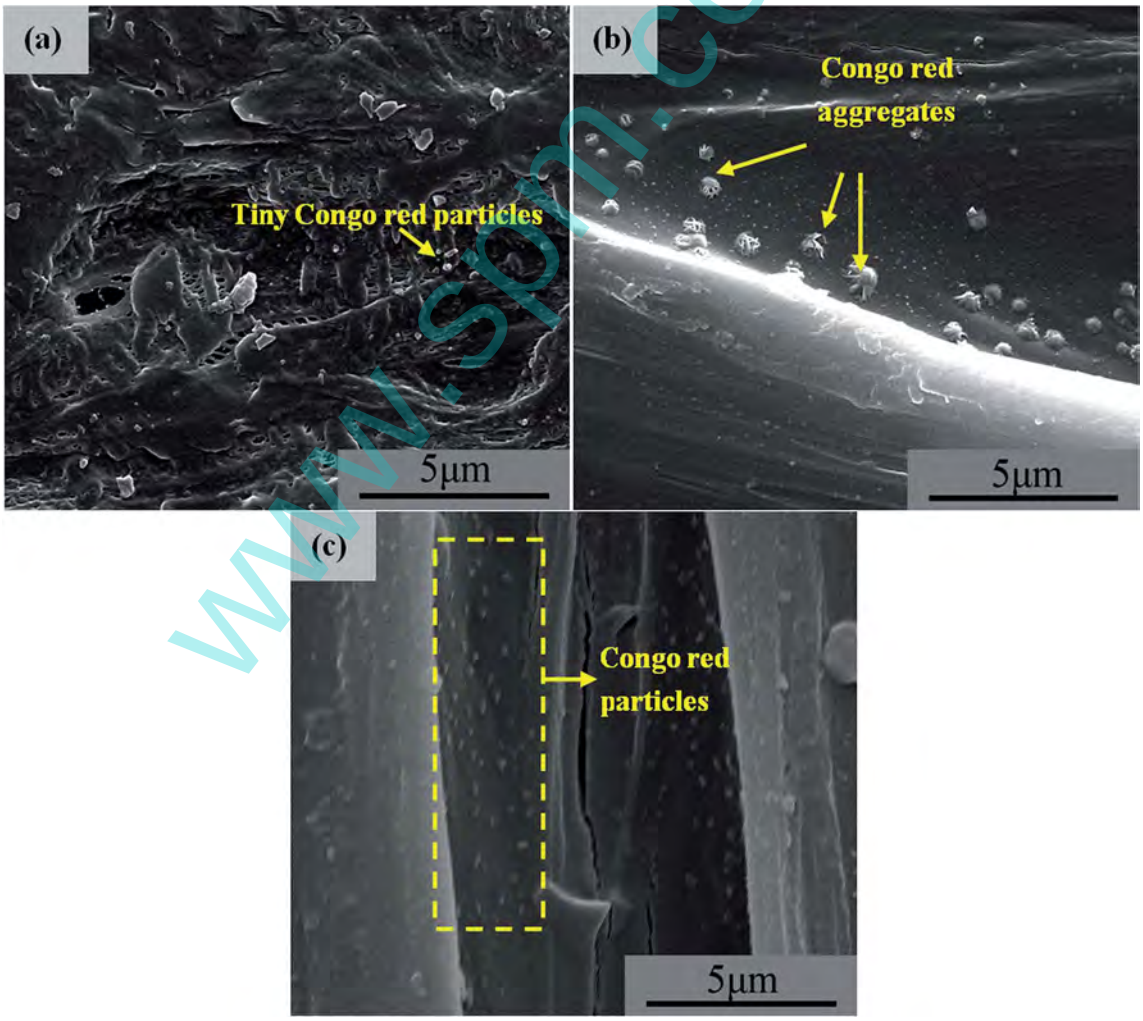

Fig. 8 SEM images showing the particle adsorption on the membrane surface of (a) M0; (b) M10; (c) M30.

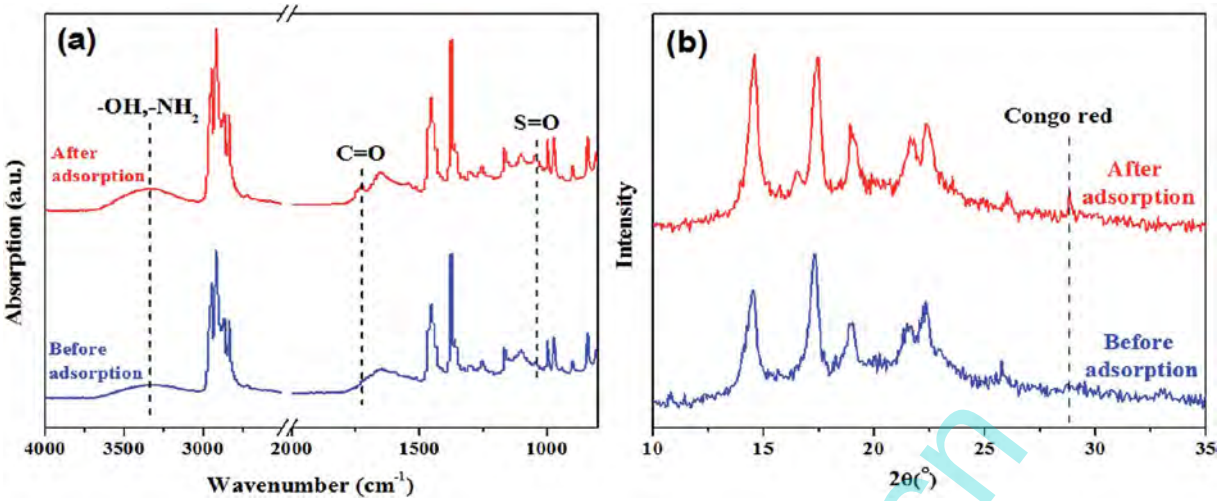

Fig. 9 (a) FTIR spectra and (b) WAXD profiles of PP composite membrane before and after adsorbing Congo red particles. The composite membranes were first treated through plasma assisted surface modification and the discharging time was 30 min during the surface modification process.

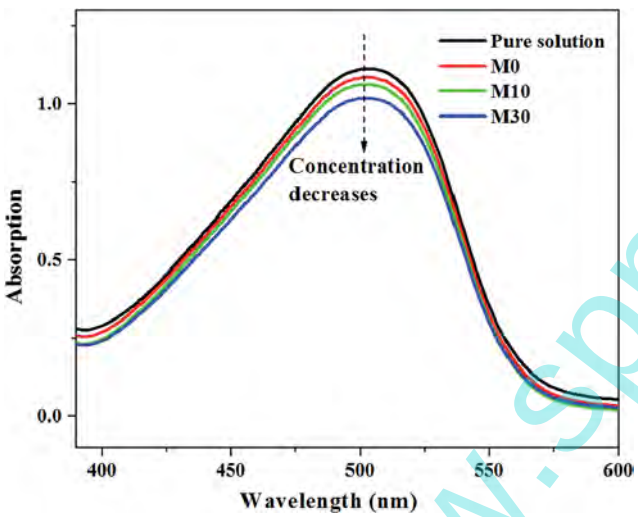

Fig. 10 UV-Vis curves showing the concentration of residual Congo red particles in the solvent after adsorption.

facilitates the adsorption of Congo red particles on the composite membrane. Consequently, amounts of Congo red aggregates can stably adhere to the membrane surface. Furthermore, one can see that increasing discharge time during the plasma treatment results in the formation of more functional groups on the composite membrane and consequently, more Congo red particles with smaller size are adsorbed on the membrane surface as shown in Fig. 8c due to the increase of the adsorption sites.

In order to confirm the results, the membranes obtained before and after adsorbing Congo red particles were comparatively investigated using FTIR and WAXD. As shown in Fig. 9a, compared with the FTIR spectrum of membrane before adsorption, the membrane after adsorption exhibits a stretching vibration of S=O group (1044 cm^{-1}) and the intensified stretching vibration of $-NH_2$ and/or –OH groups (3335 cm^{-1}), which demonstrate that Congo red particles are adsorbed on the surface of PP composite membrane. Furthermore, one can see that the stretching vibration of –C=O group becomes more apparent and shifts to higher wavenumbers, which further demonstrates that there is a strong interaction between composite membrane and Congo red particles. As shown in Fig. 9b, after adsorption, the composite membrane exhibits a characteristic diffraction peak at $2\theta = 29.9°$, attributing to the diffraction of Congo red crystals.[46] This clearly demonstrates the presence of Congo red particles on the surface of PP composite membrane.

The solutions after adsorption were also detected using UV-Vis. As shown in Fig. 10, the characteristic absorption peak of Congo red is located at the wavelength of about 500 nm. For the pure solution, the highest absorption intensity is obtained. After the adsorption with different membranes, the intensities of UV-Vis absorption peaks for the residue solutions become weaker as the discharge time of adsorptive membranes increases. That is, the Congo red concentration in solution becomes smaller, which confirms the result that more Congo red particles are adsorbed on the membrane surface with increasing the discharge time. More visualized schematic representations showing the plasma assisted surface modification of PP composite membrane and the adsorption of the treated membrane for Congo red particles are illustrated in Fig. 11.

To better understand the adsorption ability of the modified PP composite membrane, the adsorption amount of Congo red particles obtained in this work is compared with other materials (absorbents) reported in the literatures.[47–54] As shown in Fig. 12, the modified PP composite membrane exhibits the adsorption amount of about 500 mg g^{-1}, which is slightly lower than the 560 mg g^{-1} of carbon nanotubes (CNTs)/graphene aerogel but apparently higher than those of the other absorbents. This clearly demonstrates that the modified PP composite

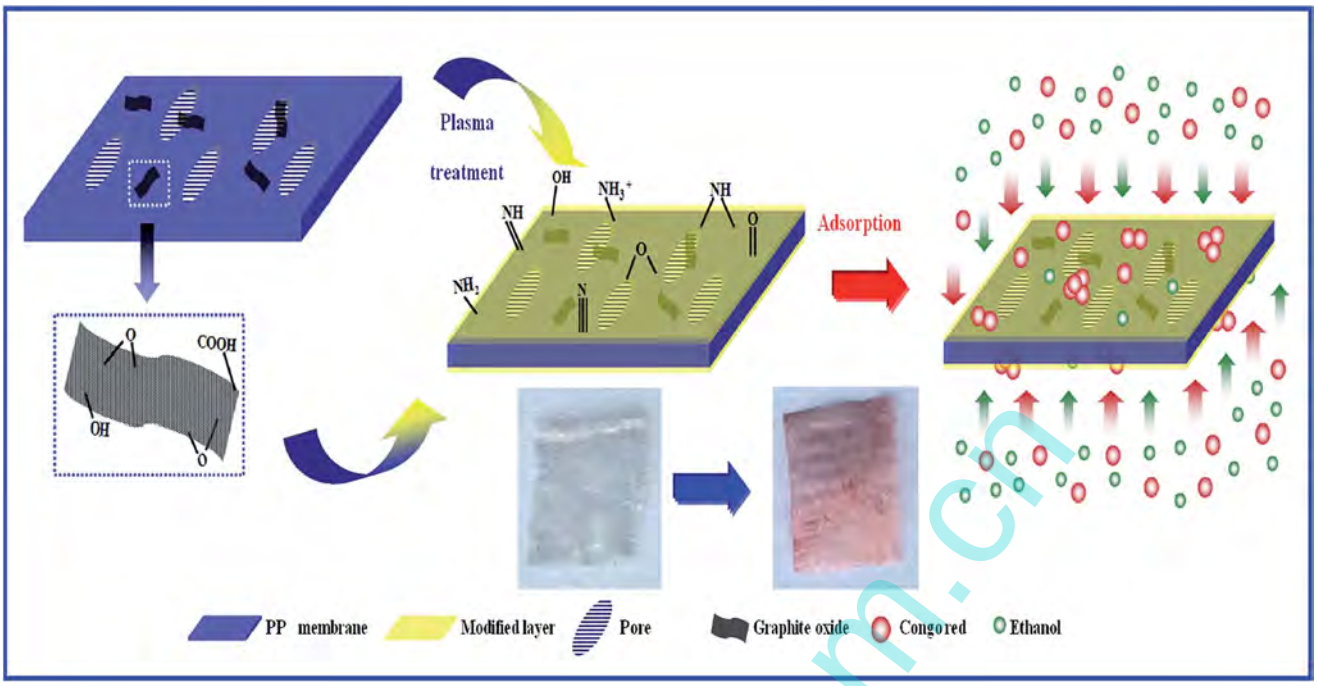

Fig. 11 Schematic representations showing the plasma assisted surface modification and the adsorption of Congo particles on the surface of treated PP composite membranes.

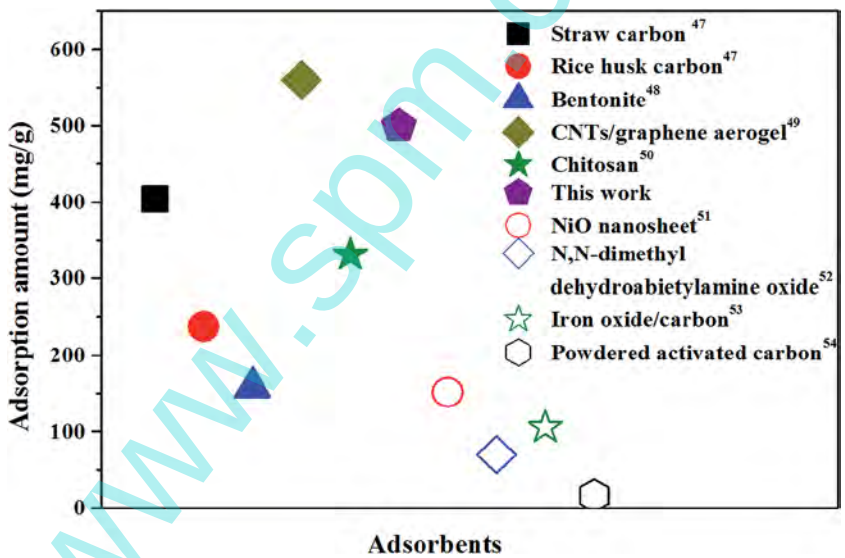

Fig. 12 Comparison of absorption amounts of Congo red particles absorbed by different absorbents between the treated PP composite membrane and those absorbents reported in the literatures.[47–54]

membrane exhibits excellent adsorption ability. Obviously, with the results above, it can be concluded that the plasma treatment technology endows the PP/GO/OP-10 membrane with useful functions and the treated porous composite membrane has a great potential in particle adsorption, which is in favor of wastewater treatment. More work will be carried out to investigate the removal of adsorbed Congo red particles from the composite membrane to understand the reusability of the composite membrane and the selective adsorption ability of the composite membrane for various organic dyestuffs.

4. Conclusions

A novel method of the allylamine plasma assisted surface modification technology has been developed for preparing a PP-based porous composite membrane with the high-hydrophilicity and the excellent adsorption ability. The results show that the excellent hydrophilicity is successfully achieved because a functional layer containing amounts of N- and O-containing functional groups are deposited on the surface of the composite membrane after the plasma treatment process.

The porosity of the porous membrane gradually decreases with increasing discharge time. The adsorption ability measurement for particles in solution has also been carried out, and the results demonstrate that Congo red particles can be adsorbed on the porous composite membrane and the adsorption capacity increases with increasing the discharge time. It is suggested that the weakened interaction between Congo red particles and ethanol solvent and the stable interaction between Congo red particles and O-containing groups on the membrane surface mainly contribute to the excellent adsorption ability of the treated composite membrane. Obviously, this work provides a highly effective and environmental-friendly method to apparently improve the hydrophilicity and adsorption ability of PP-based composite membrane with great potential in the field of wastewater treatment.

Acknowledgements

Authors express their sincere thanks to the National Natural Science Foundation of China (51173151) and Distinguished Young Scholars Foundation of Sichuan (2012JQ0057) for financial support.

References

1 F. Farjadian, S. Schwark and M. Ulbricht, *Polym. Chem.*, 2015, **6**, 1584.
2 L. Wu, J. P. Zhang, B. C. Li and A. Q. Wang, *Polym. Chem.*, 2014, **5**, 2382.
3 W. J. Cloete, C. Adriaanse, P. Swart and B. Klumperman, *Polym. Chem.*, 2011, **2**, 1479.
4 T. Y. Liu, R. X. Zhang, Q. Li, B. V. D. Bruggen and X. L. Wang, *J. Membr. Sci.*, 2014, **472**, 119.
5 W. P. Zhu, S. P. Sun, J. Gao, F. J. Fu and T. S. Chung, *J. Membr. Sci.*, 2014, **456**, 117.
6 D. J. Upadhyay and N. V. Bhat, *Plasmas Polym.*, 2003, **8**, 237.
7 S. Panmasundaram, J. H. Jung, E. Chung, S. K. Maeng, S. H. Lee, K. G. Song and S. W. Hong, *Carbon*, 2014, **70**, 179.
8 G. T. Offord, S. R. Armstrong, B. D. Freeman, E. Baer, A. Hiltner and D. R. Paul, *Polymer*, 2013, **54**, 2796.
9 C. Feng and K. Yoshiharu, *Polymer*, 1996, **37**, 573.
10 J. Dai, X. H. Liu, J. H. Yang, N. Zhang, T. Huang, Y. Wang and Z. W. Zhou, *Compos. Sci. Technol.*, 2014, **99**, 59.
11 V. Goodarzi, S. H. Jafari, H. A. Khonakdar, B. Ghalei and M. Mortazavi, *J. Membr. Sci.*, 2013, **445**, 76.
12 S. H. Tabatabaei, P. J. Carreau and A. Ajji, *J. Membr. Sci.*, 2009, **345**, 148.
13 S. H. Tabatabaei, P. J. Carreau and A. Ajji, *J. Membr. Sci.*, 2008, **325**, 772.
14 B. Jung, *J. Membr. Sci.*, 2004, **229**, 129.
15 E. Gorouhi, M. Sadrzadeh and T. Mohammadi, *Desalination*, 2006, **200**, 319.
16 Q. Xu, J. Yang, J. Dai, Y. Yang, X. Q. Chen and Y. Wang, *J. Membr. Sci.*, 2013, **448**, 215.
17 A. Saffar, P. J. Carreau, M. R. Kamal and A. Ajji, *Polymer*, 2014, **55**, 6069.
18 Y. F. Yang, L. S. Wan and Z. K. Xu, *J. Membr. Sci.*, 2009, **326**, 372.
19 C. Q. Zhao, X. C. Xu, R. Y. Li, J. Chen and F. L. Yang, *Water Sci. Technol.*, 2013, **67**, 2307.
20 A. Saffar, P. J. Carreau, A. Ajji and M. R. Kamal, *J. Membr. Sci.*, 2014, **462**, 50.
21 T. C. Chung and S. H. Lee, *J. Appl. Polym. Sci.*, 1997, **64**, 567.
22 Q. Yang, Z. K. Xu, Z. W. Dai, J. L. Wang and M. Ulbricht, *Chem. Mater.*, 2005, **17**, 3050.
23 Z. K. Xu, J. L. Wang, L. Q. Shen, D. F. Men and Y. Y. Xu, *J. Membr. Sci.*, 2002, **196**, 221.
24 S. C. Yu, Y. P. Zheng, Q. Zhou, S. Shuai, Z. H. Lv and C. J. Gao, *Desalination*, 2012, **298**, 49.
25 M. X. Hu, Q. Yang and Z. K. Xu, *J. Membr. Sci.*, 2006, **285**, 196.
26 E. M. Liston, L. Martinu and M. R. Wertheimer, *J. Adhes. Sci. Technol.*, 1993, **7**, 1091.
27 B. Jaleh, P. Parvin, P. Wanichapichart, A. P. Saffar and A. Peyhani, *Appl. Surf. Sci.*, 2010, **257**, 1655.
28 J. A. Franco, D. D. Demontigny, S. E. Kentish, J. M. Perera and G. W. Stevens, *Ind. Eng. Chem. Res.*, 2012, **51**, 1376.
29 Y. F. Yang, L. S. Wan and Z. K. Xu, *J. Membr. Sci.*, 2009, **337**, 70.
30 J. Zhou, W. Zhou, J. S. Gu and H. Y. Yu, *Membr. Water Treat.*, 2010, **1**, 83.
31 H. Chen, Q. Lin, Q. Xu, Y. Yang, Z. P. Shao and Y. Wang, *J. Membr. Sci.*, 2014, **458**, 217.
32 J. Dai, X. L. Xu, J. H. Yang, N. Zhang, T. Huang, Y. Wang, Z. W. Zhou and C. L. Zhang, *RSC Adv.*, 2015, **5**, 20663.
33 S. Hummers and R. E. Offeman, *J. Am. Chem. Soc.*, 1958, **80**, 1339.
34 J. H. Yang, C. X. Feng, J. Dai, N. Zhang, T. Huang and Y. Wang, *Polym. Int.*, 2013, **62**, 1085.
35 A. Abbas, C. Vivien, B. Bocquet, D. Guillochon and P. Supiot, *Plasma Processes Polym.*, 2009, **6**, 593.
36 J. R. Hollahan and T. Wydeven, *Science*, 1973, **179**, 500.
37 S. J. Liu, C. X. Zhou and W. Yu, *J. Membr. Sci.*, 2011, **379**, 268.
38 Z. L. Yang, X. N. Wang, J. Wang, Y. Yao, H. Sun and N. Huang, *Plasma Processes Polym.*, 2009, **6**, 498.
39 Z. L. Yang, J. Wu, X. Wang, J. Wang and N. Huang, *Plasma Processes Polym.*, 2012, **9**, 718.
40 P. Hamerli, T. Weige, T. Groth and D. Paul, *Biomaterials*, 2003, **24**, 3989.
41 P. Hohenberg, *Phys. Rev.*, 1964, **136**, 864.
42 B. M. Ganesh, A. M. Isloor and A. F. Ismai, *Desalination*, 2013, **313**, 199.
43 T. F. Wu, B. M. Zhou, T. Zhu, J. Shi, Z. W. Xu, C. S. Hu and J. J. Wang, *RSC Adv.*, 2015, **5**, 7880.
44 F. Zuo, J. K. Keum, X. M. Chen, B. S. Hsiao, H. Y. Chen, S. Y. Lai, R. Wevers and J. Li, *Polymer*, 2007, **48**, 6867.
45 G. T. Offord, S. R. Armstrong, B. D. Freeman, E. Baer, A. Hiltner, J. S. Swinnea and D. R. Paul, *Polymer*, 2013, **54**, 2577.
46 S. Y. Liu, Y. Cai, X. Y. Cai, H. Li, F. Zhang, Q. Y. Mu, Y. J. Liu and Y. D. Wang, *Appl. Catal., A*, 2013, **453**, 45.
47 N. Kannan and M. Meenakshisundaram, *Water, Air, Soil Pollut.*, 2002, **138**, 289.
48 E. Bulut, M. Özacar and İ. A. Şengil, *J. Hazard. Mater.*, 2008, **154**, 613.

49 B. Lee, S. Lee, M. Lee, D. H. Jeong, Y. Baek, J. Yoon and Y. H. Kim, *Nanoscale*, 2015, **7**, 6782.
50 L. Wang and A. Wang, *Bioresour. Technol.*, 2008, **99**, 1403.
51 B. Cheng, Y. Le, W. Cai and J. Yu, *J. Hazard. Mater.*, 2011, **185**, 889.
52 S. Liu, Y. Ding, P. Li, K. Diao, X. Tan, F. Lei, Y. Zhan, Q. Li, B. Huang and Z. Huang, *Chem. Eng. J.*, 2014, **248**, 135.
53 T. Hao, X. Rao, Z. Li, C. Niu, J. Wang and X. Su, *J. Alloys Compd.*, 2014, **617**, 76.
54 Y. Fu and T. Viraraghavan, *Adv. Environ. Res.*, 2002, **7**, 239.